

UDC 528.21

CONTRIBUTION OF AEROGRAVITY DATA INTERPRETATION TO THE STUDY OF THE DEEP STRUCTURE OF AGADEM PETROLEUM BLOCK (NIGER)

Abdourhamane HALIDOU AMADOU^{✉*}, Driss EL AZZAB, Abdel Ali CHAOUNI

*Intelligent Systems Georesources and Renewable Energy Laboratory, Faculty of Science and Technology,
Sidi Mohamed Ben Abdallah University, BP: 2202, Imouzzar Road, Fez, Morocco*

Received 19 September 2022; accepted 15 September 2023

Abstract. The main information provided by gravity maps is the geographical distribution of density heterogeneities in the subsurface. It is an important tool widely used for the mapping of geological structures, especially in the oil industry. Thus, this study based on the interpretation of aerogravity data has for objective, the qualitative description of the characteristics of the gravity anomalies of the study area, interpretation and mapping of the gravity lineaments as well as their depths, knowing that the lineaments constitute potential structural traps favorable to the accumulation of the hydrocarbons. Methods such as horizontal derivative, upward continuation and Euler deconvolution are used to give a geological significance to the different anomalies and to highlight deep structures. Thus, the analysis of the residual anomaly map revealed elongated negative and positive anomaly zones, oriented globally NW-SE, considered respectively as horst and graben zones. Gravity lineaments, considered as normal faults, are mapped using the horizontal gradient method. Finally, the depths of the density contrasts are estimated by the Euler deconvolution calculation using the value “1” as structural index. The depths thus determined are highly variable. The shallowest depths vary between 3000 m and 6000 m, while the deepest depths reach 18000 m.

Keywords: gravity, structural, interpretation, anomalies, lineaments, Agadem Block.

Introduction

The successful development of an airborne gravity meter has long been a challenge for exploration geophysicists and serious consideration of the subject probably dates back to the time of the introduction of the airborne magnetometer, as gravity and magnetic methods are potential technical areas (Hood & Ward, 1969). According to Hammer (1982), a special survey, to permit direct comparison of airborne and conventional ground gravity data, was made in August, 1981, in the Texas Gulf Coast. It has been observed that the accuracy and resolution of anomalies obtained from airborne gravity data are twice as good as those from conventional gravity data. Airborne geophysical techniques have been found to be effective in delineating surface and subsurface features, and, when used in conjunction with other exploration techniques, become an important tool for developing a comprehensive geological model (Armstrong & Rodeghiero, 2006). The airborne gravity was so integral to oil exploration that from 1930 to 1935, the total number of gravity crews exceeded the total number of seismic crews (Nabighian et al., 2005).

According to Dampney (2018), gravity interpretation can play two important roles in petroleum exploration: determining the nature and structure of the sedimentary basin basement and detailing important local tectonic features, such as salt domes, volcanic intrusions and faults.

Our study area is located between latitude 14°30'–17°00' N and longitude 12°00'E–14°00' E and constitutes the main part of the Termit basin. It covers an area of about 27000 km². In the early 1960s, the Office de la Recherche Scientifique et Technique Outre-Mer (ORSTOM) conducted the first gravity surveys, through the program West and Central African gravity surveys. Subsequently, numerous aero-geophysical surveys were carried out from 1970 to 2015. In 2015, the Agadem block was the subject of aero-geophysical surveys carried out by ARKeX Ltd company. This is the most recent aero-geophysical survey in the area. These data are used in this study to analyse and interpret the characteristics of gravity anomalies, to identify and map gravity lineaments and to estimate the depths of density contrasts. However, several methods such as upward continuation, horizontal gradient and Euler

*Corresponding author. E-mail: abdourhamane.halidou@usmba.ac.ma

deconvolution were used to facilitate the interpretation of the data.

1. Geographical location of the study area

The Agadem Block is located within the southeast of Niger Republic, about 1400 km from the capital Niamey. It covers most of the Termit sedimentary basin with an area of approximately 27 516 km² and is 300 km long from N-S and 60 to 110 km wide from E-W. It is located by the coordinates 14° 30'–17° 00' N and 12° 00'–14° 00' E (Figure 1). Topographically, the Agadem Block lies at the southern edge of the Sahara desert at an altitude between 270 and 470 m above sea level, with a generally high relief in the NW and a depression in the SE. The variable topography is mainly due to the formation of sand dunes in the form of waves. Despite the dry climate and the sparse vegetation, the area is rich in groundwater with aquifers lying less than 100 m deep.

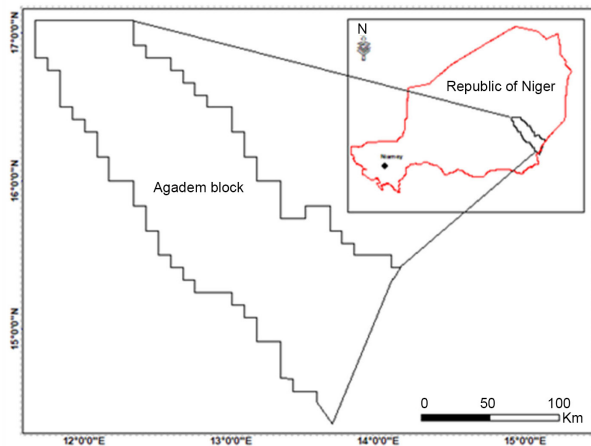


Figure 1. Geographical location of Agadem block

2. Materials and methods

2.1. Geological and tectonic framework of Termit basin

Located in the border region of Niger and Chad (Figure 2), the Termit basin is an asymmetric extensional NW-SW-trending rift, about 600 km long and 150–200 km wide (Guiraud & William, 1997). It is part of the Cretaceous-Paleogene rifts system make up a geotectonic continuum termed the West and Central African Rift System (WCARS) that extends 4000 km from the Gao trough in Mali to the Anza basin in Kenya (Fairhead, 1988a). The origin of WCARS is generally attributed to the breakup of Gondwana and the opening of the South Atlantic Ocean and Indian Ocean starting about 130 Ma (Ajakaiye & Burke, 1973; Fairhead, 1980; Guiraud, 1990).

According to Genik (1992), this rift system is subdivided into two coeval Cretaceous genetically related but physically separated: the West African Rift Subsystem (WARS) and Central African Rift Subsystem (CARS). Genik (1993) considers that the evolution of the WCARS was accompanied by a generally low level of magmatic activity. Geophysical studies of the crustal and lithospheric structure of the WCARS basins conducted by Wilson (1992) indicate that these subsided in response to large amounts of crustal extension.

In WCARS, the Cretaceous rifts are associated with large crustal extension resulting in major crustal thinning which has dominated the isostatic response resulting in surface subsidence (Fairhead, 1988b; Fairhead & Green, 1989). Thus, two major rifting stages are evident: the first one is Early Cretaceous in age and is characterised by large NW-SE-trending fault blocks; the second one is late Senonian-Paleogene and is represented by NNW-SSE-trending normal faults (Guiraud & Maurin, 1992).

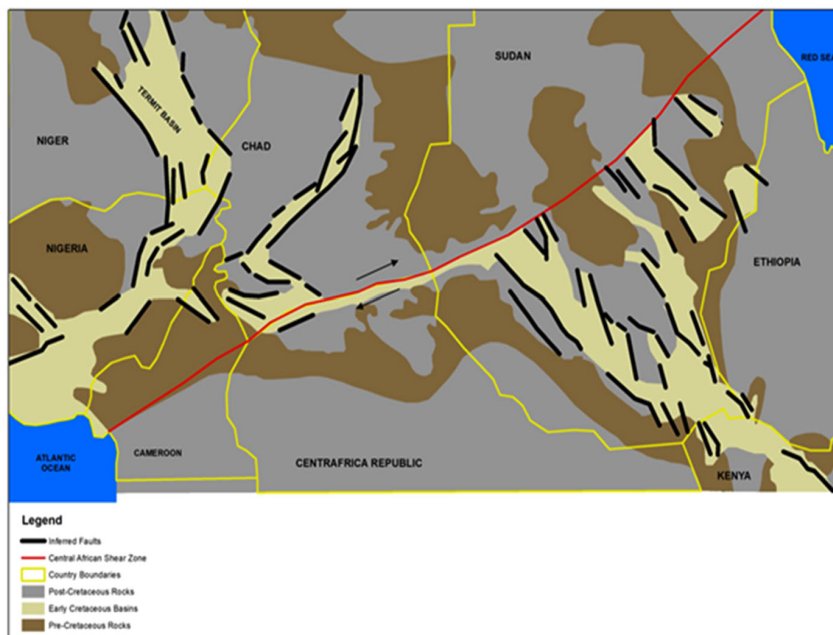


Figure 2. West and Central Africa Rift System (modified from Fairhead, 1988b)

Precambrian basement

It consists of biotite gneiss, pegmatite, quartz mica schist, phyllite, granite. The lithological components include also celadon and green ash low-grade metamorphic blastopelitic siltstone and palimpsest fine siltstone with low metamorphic grade.

Cretaceous formations

It composed of the Lower Cretaceous and Upper Cretaceous. Lithologic component of Lower Cretaceous consists of alternate layers of sandstone with kiesel, kaolinite and quartz, siltstone and mudstone. The Upper Cretaceous includes the following formations from bottom to top:

- Donga formation: consists of sandstone and gradually transits to mudstone upwards. The lower Donga consists of sandstone, mudstone, siliceous, kaolin and some quartzose clean.
- Yogou Formation: it is basically composed of argillutite, major source rock in the basin, and some local sandstone at the top. The lithological components include thick grey and dark argillutite sandwiched with grey and dark shale and thin finestone and medium sandstone.
- Madama Formation: it consists of thick sandstone widely spreading in the area and a little of thin argillaceous sandstone (with coal seams) at the top and the bottom.

Paleogene formations

The Paleogene formation is divided into two sections: Lower Sokor (Sokor1) formation which is mainly contains alternate layers of sandstone and mudstone, and upper Sokor (Sokor2) composed of lacustrine mudstone sandwiched with thin sandstone, grey and dark mudstone.

Neogene formations

It is basically composed of finestone to coarse-grain sandstone and minerals are mainly quartz and feldspar with a little of clay, which are sediments of fluvial facies.

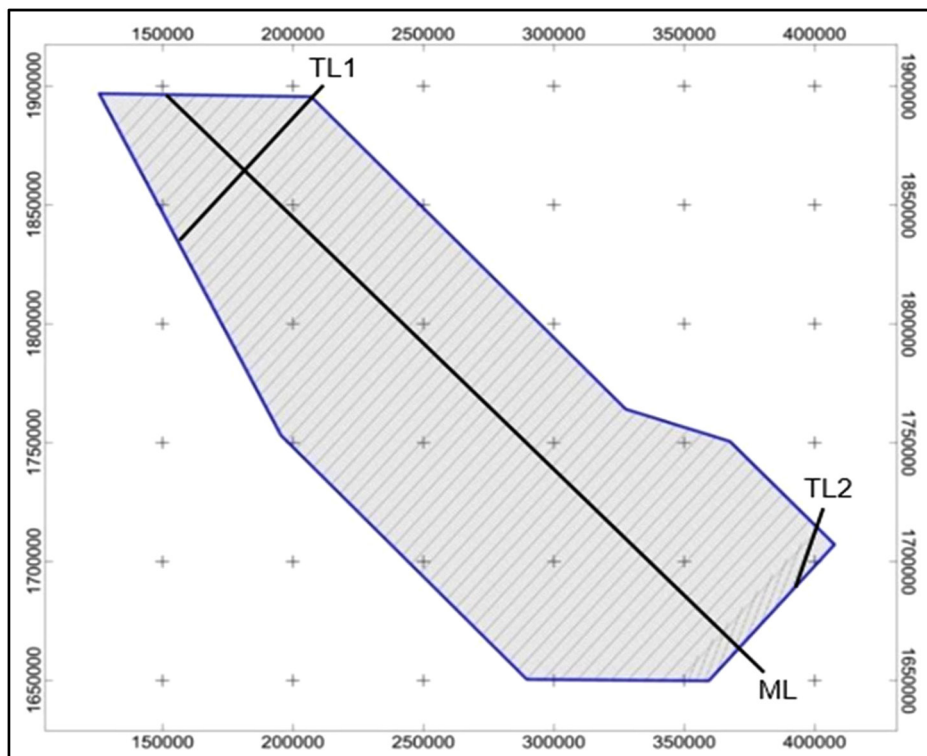
Quaternary formations

The Quaternary formation is made up of clay, siltstone, finestone and gravel beds. Its surface is covered by desert with thickness 10 m.

2.2. Data characteristics

The aerogravity data used in this study were acquired by ARKeX company at an altitude of 120 m above ground level during the period from December 2014 to February 2015. Figure 5 shows the lines of the survey plan. The flight line (main lines) spacing is 1000 m with a direction N137.5°. The tie lines were flown perpendicular to the main lines with a spacing of 5000 m oriented N40° and 3000 m in the southern infill area with a direction N20°.

The collected data are corrected for temporal spatial and drift effects and then recalculated at the nodes of a regular grid spacing of 250 m.



Note: ML: Main lines, TL: Tie lines.

Figure 5. Survey line plan (ARKeX Ltd, 2015)

2.3. Methods

In order to facilitate the interpretation of the data, several techniques such as upward continuation, horizontal gradient and Euler deconvolution were applied.

2.3.1. Upward continuation

Upward continuation is a low-pass filter which consists of calculating the shape and amplitude of an anomaly on a surface higher than the observation surface and thus allows to compare data acquired at different altitudes (Dubois et al., 2011). It is a mathematical technique which can be used to separate the anomaly of the deeper geology from shallower geology (Jacobsen, 1987). Thus, upward continuation is a method to separate a regional gravity anomaly resulting from deep sources from the observed gravity (Zeng et al., 2007).

According to Blakely and Simpson (1986) this technique consists to transform the potential field measured on one surface to the field that would be measured on another surface farther from all sources. As we shall see, this transformation attenuates anomalies with respect to wavelength; the shorter the wavelength, the greater the attenuation. Thus, this approach therefore emphasises large sources linked to relatively deep sources (El Azzab et al., 2001). In the case of our study, we applied the upward continuation to the residual anomaly map at altitudes 10000 m, 20000 m, 30000 m and 40000 m to obtain the local sources.

2.3.2. Horizontal derivative

The horizontal gradient method has been used since 1982 to locate density or magnetic boundaries from gravity data (Cordell, 1979). The method is based on the principle that a near vertical, fault-like boundary produces a gravity anomaly whose horizontal gradient

is largest directly over the top edge of the boundary (Grauch & Cordell, 1987). Horizontal gravity gradients emphasise the boundaries of upper crustal density contrasts associated with major tectonic and volcanic structures (Grieve et al., 1987). The location of these boundaries is facilitated by the calculation of the horizontal gradient of gravity (Cordell & Grauch, 1985) from the following equation:

$$f(x, y) = \sqrt{\left(\frac{\partial g}{\partial x}\right)^2 + \left(\frac{\partial g}{\partial y}\right)^2}$$

The greatest advantage of this method is its low sensitivity to noise (Basseka et al., 2016). Large horizontal gravity gradients require shallow lateral density contrasts (Hildebrand et al., 1995). For this reason, we used the residual anomaly map to highlight local maxima that represent indicators of lateral density contrasts and are interpreted as geological contacts or tectonic accidents.

2.3.3. Euler deconvolution

The standard Euler deconvolution uses three orthogonal gradients of any potential quantity to estimate the location of a source body. Theoretically, the gravity and magnetic fields caused only by pure 2D and 3D sources (e.g: line and point) satisfy Euler’s homogeneity equation exactly (Beiki, 2010). However, Reid et al. (1990) consider that in practice, this technique can be applied to the fields from causative bodies of arbitrary shapes.

However, the application of this method requires an appropriate choice of the structural index. Thus, the use of the wrong index yields scattered solutions and biased depth. An index that is too low gives depths that are too shallow; one that is too high gives estimates that are too deep (Reid et al., 1990).

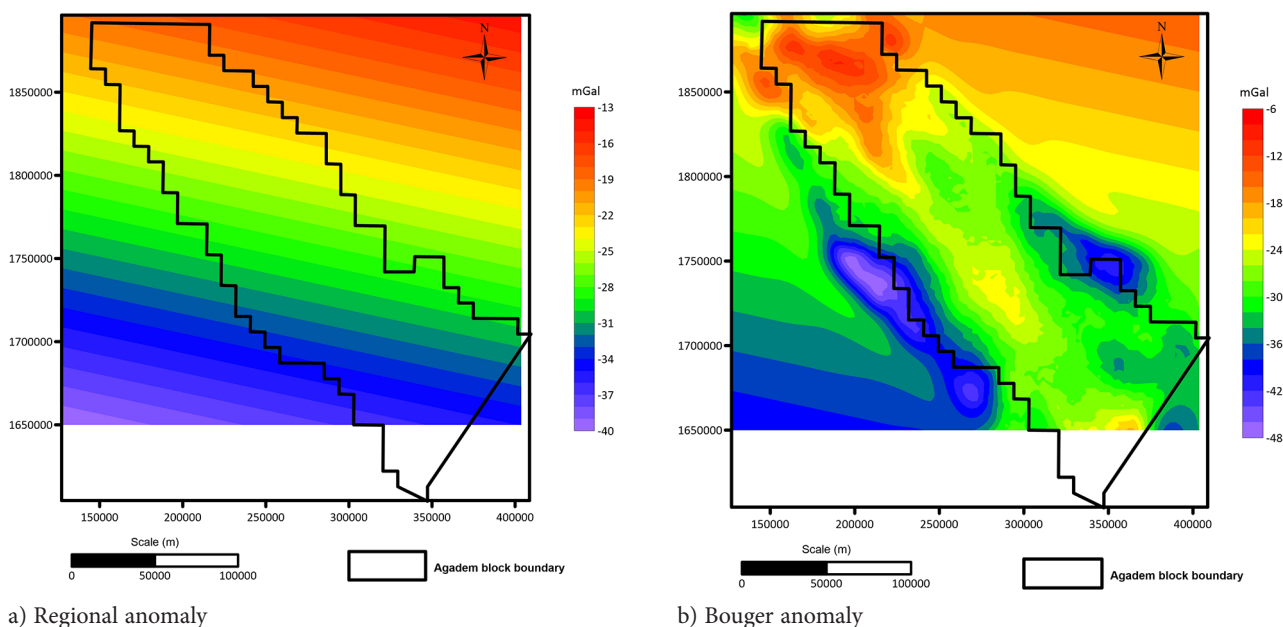


Figure 6. Map showing regional and Bouguer anomaly map

3. Results and discussion

3.1. Analysis of the residual anomaly map

The residual anomaly map was obtained by subtracting the regional field map adjusted by a low degree polynomial (Figure 6a) from the Bouguer map (Figure 6b). The residual anomaly map is very disturbed and shows positive and negative anomalies of elongated shapes oriented globally NW-SE, with values varying between -18 and 20 mGal (Figure 7). Positive anomalies of various sizes appear in the northwest and southeast. separating large negative anomalies along the eastern and western edges of Agadem block. These negative anomalies extend to the east of the block, over a length of 106 km and a width of 40 km and 86 km in length and 43 km in width to the

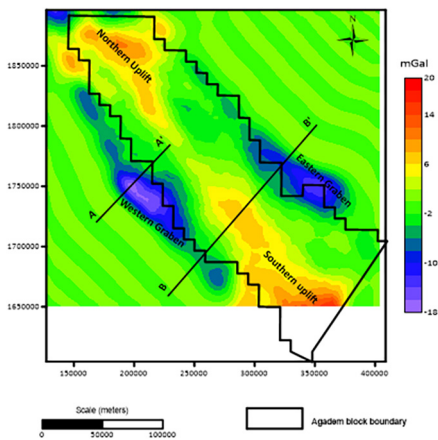


Figure 7. Residual gravity anomaly map

west. According to Fairhead (1988a), the negative gravity anomalies observed in the eastern rifts of Niger are caused by low density sediments. These negative anomalies correspond to graben zones that extend over considerable distances with a strong sedimentary filling, while the positive anomalies correspond to the uplift zones which explains the presence of a shallow basement in this area. Thus, the interpretation of the residual anomaly map from the Figure 7, allowed to highlight four (4) structural zones in the Agadem block: the North uplift zone, the South uplift zone, the East graben and the West graben.

Figures 8 and 9 illustrate the results obtained from cross-sections AA' and BB' plotted on the residual field map. These profiles, oriented NE-SW and perpendicular to the anomalies, highlight the graben and horst structures of the study area with fault locations at the points indicated by the arrows. The graben zones correspond to the areas of strong negative gravity anomaly observed on the residual field map. However, the profiles are not too disturbed and one can think that the gravity map could then be essentially dependent on the variation in thickness of the sedimentary filling.

3.2. Upward continuation interpretation

In order to highlight the deep gravity sources, an upward continuation filter was applied to the residual anomaly map, following the altitudes 10000 m, 20000 m, 30000 m and 40000 m (Figure 10). Thus, the map of upward continuation to 40000 m (Figure 10d) shows negative and positive anomalies with values between -3.5 mGal and 5 mGal. The positive anomalies merge to form a single

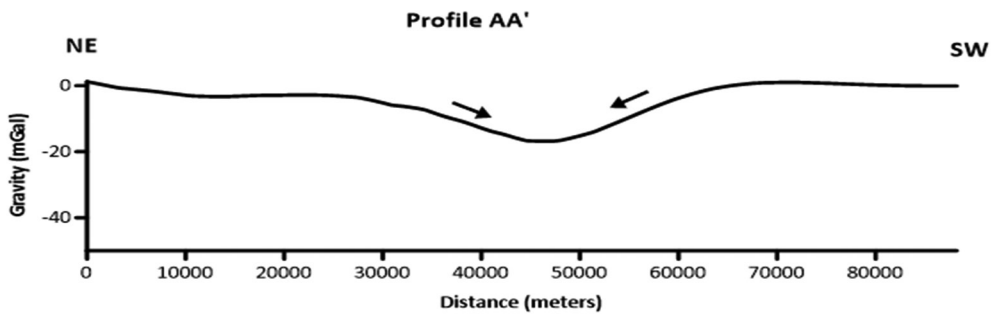


Figure 8. AA' profile of the residual gravity anomaly

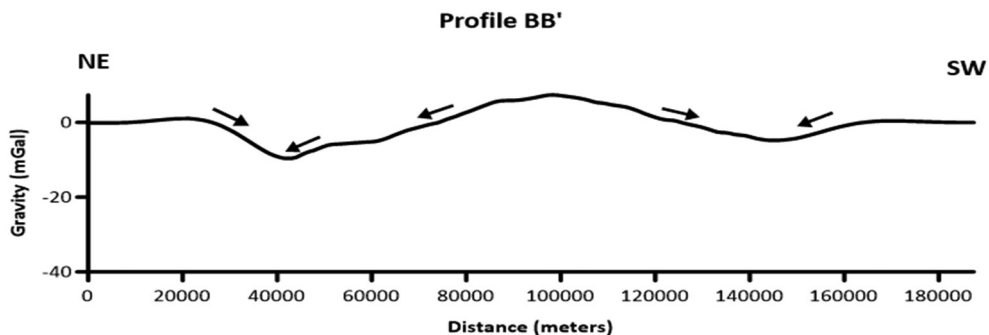


Figure 9. BB' profile of the residual gravity anomaly

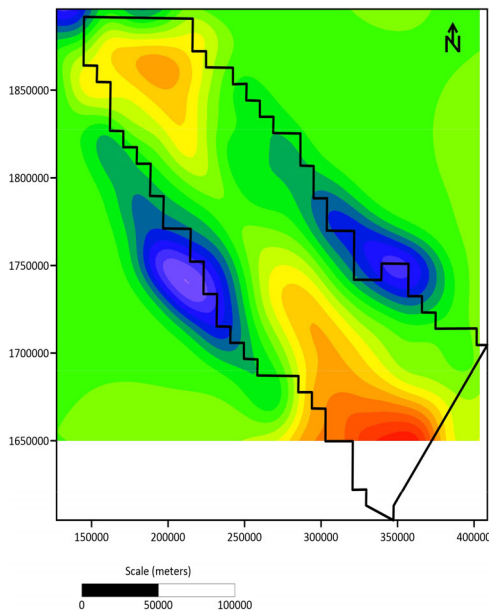
anomaly occupying the SE part of the block. Whereas, negative anomalies occupy the NW half of the study area with regular oval shapes oriented along the NW-SE direction. However, despite the various upward extensions, negative anomalies located at the eastern and western edges of the block persist. This could be explained by the existence in these areas of depressed zones with a strong sedimentary filling.

3.3. Horizontal derivative

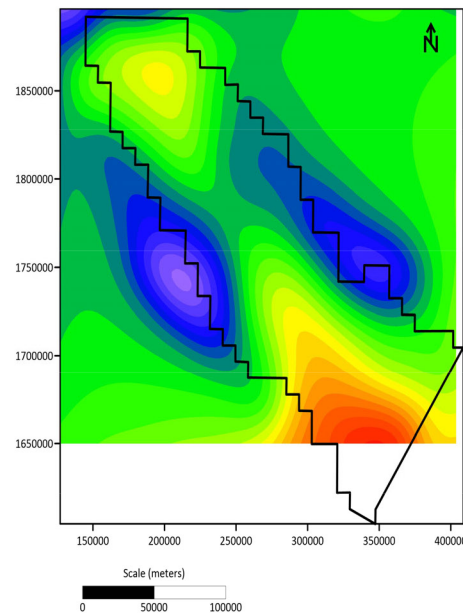
It has long been recognised that the most convincing method of identifying gravimetric lineaments is incontestably

the horizontal gradient method. The Figure 11 shows the gravity lineaments deduced from the residual anomaly map by the horizontal derivative method. We can see that lineaments are globally oriented following the NW-SE direction. However, there are lineaments that are also oriented WNW-ESE, NNW-SSE and E-W (Figure 12).

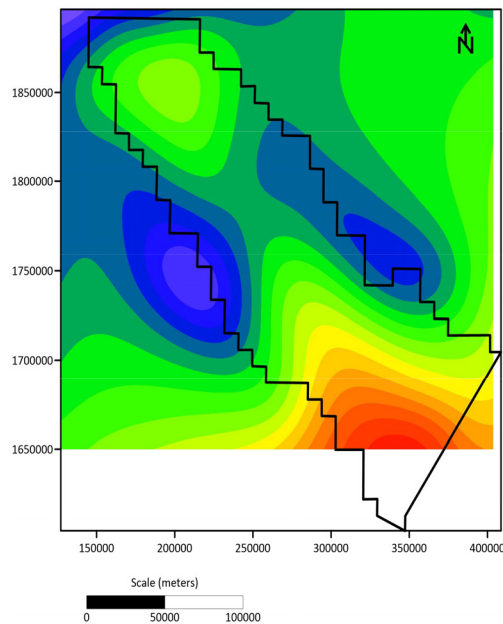
By superimposing gravity lineaments identified on the geological map (Figure 13), there is a perfect compatibility between the major structural direction of the area represented by the seismic faults and the orientation of the lineaments. This affinity between the two directions confirms the close relationship between the emplacement



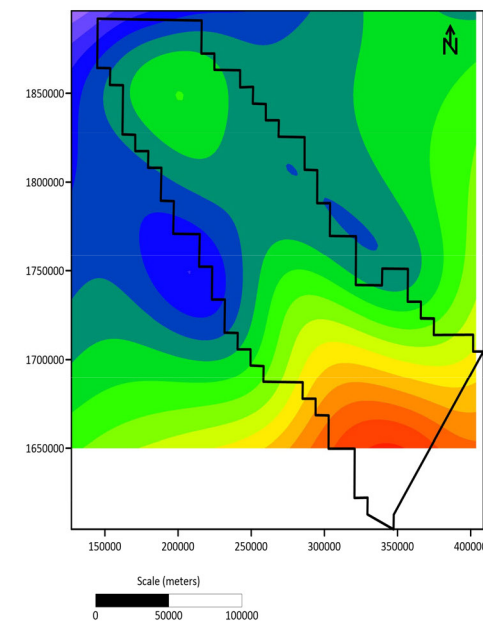
a) Upward continuation to 10000 m



b) Upward continuation to 20000 m



c) Upward continuation to 30000 m



d) Upward continuation to 40000 m

Figure 10. Upward continuation of the residual gravity anomaly map

of the gravity anomalies and the fracturing that affected the area during the Lower Cretaceous rifting period when large NW-SE fault blocks were emplaced (Guiraud et al., 1987).

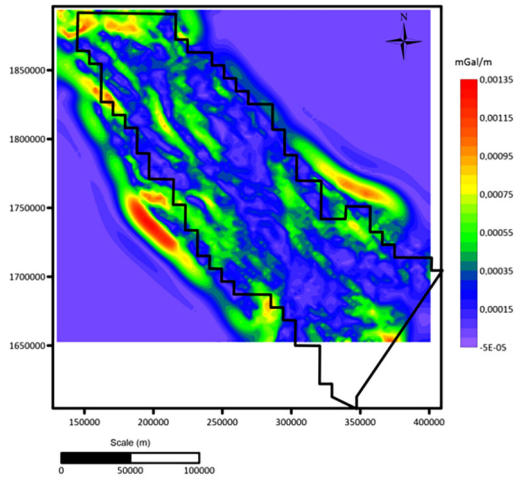


Figure 11. Horizontal gradient of the residual gravity anomaly map

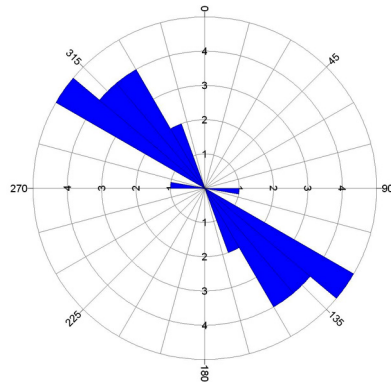


Figure 12. Diagram of fractures distribution

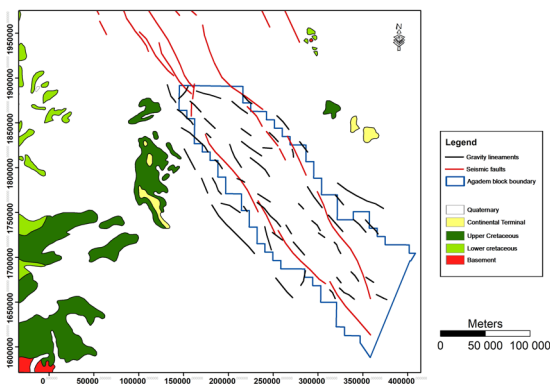


Figure 13. Gravity lineaments superimposed on the geological map

3.4. Euler deconvolution

The determination of the depths of gravity lineaments was possible through the calculation of the Euler deconvolution. In fact, the efficacy of this method depends on the

choice of the structural index. However, in order to better represent the depths of the density contacts over the whole study area, a structural index with a value of “1” was used. Because useful structural indices for gravity anomalies are likely to lie in the range from zero to 1 (Reid et al., 1990). The Figure 14 illustrates the estimated density contrast depths. We can see that the depths of the deepest faults exceed 18000 m, while the shallowest contacts are situated between 3000 and 6000 m depth. It can be observed on the same figure that the shallower contacts are located in the NW and a part in the SE of the block. However, the deepest tectonic faults are observed to the SW corresponding to the sag zones as shown on the residual gravity anomaly map.

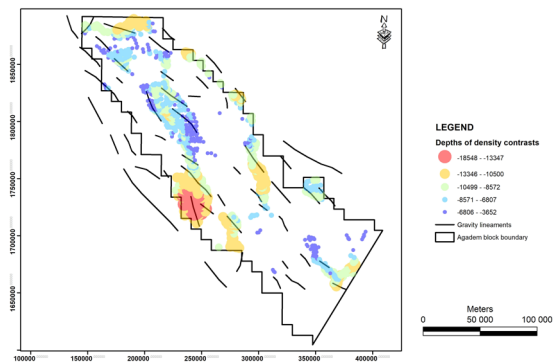


Figure 14. Density contrasts depth estimation

Conclusions

The qualitative interpretation of the residual anomaly map of Agadem block allowed to formulate the two mechanical hypotheses of the formation of sedimentary basins in relation to the gravity anomalies: extension, which leads to a negative anomaly forming grabens, and compression, which causes the rise of the basement with the development of horsts. The use of methods such as upward extension, horizontal gradient and Euler deconvolution has been helpful in studying the behaviour of gravity anomalies. The horizontal gradient map allowed the elaboration of a structural map providing a regional overview of the lengths and orientations of gravity lineaments. The main tectonic accidents oriented NW-SE, NNW-SSE and E-W are superimposed on the geological map, showing their concordance with the major structural direction of the study area. Finally, the calculation of the Euler deconvolution made it possible to determine the depths of the variable density contrasts over the entire Agadem block. Deeper density sources are observed in the southwest of the block, with values reaching 18000 m. On the other hand, the shallowest depths are globally located to the northwest.

References

Ajakaiye, D. E., & Burke, K. (1973). A Bouguer gravity map of Nigeria. *Tectonophysics*, 16, 103–115.
[https://doi.org/10.1016/0040-1951\(73\)90134-0](https://doi.org/10.1016/0040-1951(73)90134-0)

- ARKeX Ltd Company. (2015). *ARKeX data processing report*. Agadem Block.
- Armstrong, M., & Rodeghiero, A. (2006). Airborne geophysical techniques in Aziz. In *Coal Operators' Conference* (pp. 113–131), University of Wollongong and the Australasian Institute Mining and Metallurgy.
- Basseka, C. A., Nijiteu, T. C. D., Eyike, Y. A., Shandini, Y., & Kenfack, J. V. (2016). Apport des données magnétiques de surface et satellitaires à l'étude des structures profondes du Sud-Cameroun. *Sciences, Technologies et Développement*, 18, 15–30.
- Beiki, M. (2010). Analytic signals of gravity gradient tensor and their application to estimate source location. *Geophysics*, 75(6), 159–174. <https://doi.org/10.1190/1.3493639>
- Blakely, R. J., & Simpson, R. W. (1986). Approximating edges of source bodies from magnetic or gravity anomalies. *Geophysics*, 51(7), 1494–1498. <https://doi.org/10.1190/1.1442197>
- Cordell, L. (1979). Gravimetric expression of graben faulting in Santa Fe country and the Espanola basin, New Mexico. In *New Mexico Geological Society 30th Annual Fall Field Conference Guidebook, Santa Fe Country* (pp. 59–64). https://nmgsl.nmt.edu/publications/guidebooks/downloads/30/30_p0059_p0064.pdf
- Cordell, L., & Grauch, V. J. S. (1985). *Mapping basement magnetization zones from aeromagnetic data in the San Juan basin, New Mexico*. <https://doi.org/10.1190/1.0931830346.ch16>
- Dampney, C. N. G. (2018). Gravity interpretation for hydrocarbon exploration? A workshop manual or learning to see geology in a gravity profile. *Exploration Geophysics*, 8(4), 161–180. <https://doi.org/10.1071/EG977161>
- Dubois, J., Diament, M., & Cogné, J. (2011). *La gravimétrie en mer* (4e ed). Institut océanographique.
- El Azzab, D., Younés, G., & Christian, H. (2001). Contribution du géomagnétisme à l'étude géologique de la région d'aguelmouss (Est du massif hercynien central marocain). *Communications, PANGEA*, (35/36), 59–66.
- Fairhead, J. D. (1980). The Structure of the cross-cutting volcanic chain of northern Tanzania and its relation to the east african rift system. *Tectonophysics*, 65, 193–208.
- Fairhead, J. D. (1988a). Late Mesozoic rifting in Africa. *Developments in Geotectonics*, 22, 821–831. <https://doi.org/10.1016/B978-0-444-42903-2.50038-5>
- Fairhead, J. D. (1988b). Mesozoic plate tectonic reconstructions of the central South Atlantic Ocean: The role of the West and Central African Rift System. *Tectonophysics*, 155, 181–191. [https://doi.org/10.1016/0040-1951\(88\)90265-X](https://doi.org/10.1016/0040-1951(88)90265-X)
- Fairhead, J. D., & Green, C. M. (1989). Controls of rifting in Africa and the regional tectonic model for the Nigeria and East Niger rift basins. *Journal of African Earth Sciences*, 8(2–4), 231–249. [https://doi.org/10.1016/S0899-5362\(89\)80027-2](https://doi.org/10.1016/S0899-5362(89)80027-2)
- Genik, G. J. (1992). Regional framework, structural and petroleum aspects of rift basins in Niger, Chad and the Central African Republic (C.A.R.). *Tectonophysics*, 213, 169–185. [https://doi.org/10.1016/0040-1951\(92\)90257-7](https://doi.org/10.1016/0040-1951(92)90257-7)
- Genik, G. J. (1993). Petroleum geology of Cretaceous-Tertiary rift basins in Niger, Chad and Central African Republic. *The American Association of Petroleum Geologists Bulletin*, 77(8), 1405–1434. <https://doi.org/10.1306/BDF8EAC-1718-11D7-8645000102C1865D>
- Grauch, V. J. S., & Cordell, L. (1987). Short note limitations of determining density or magnetic boundaries from the horizontal gradient of gravity or pseudogravity data. *Geophysics*, 52(1), 118–121. <https://doi.org/10.1190/1.1442236>
- Grieve, R. A., Thomas, M. D., & Halpenny, J. F. (1987). Horizontal gravity gradient: An aid to the definition of crustal structure in North America. *Geophysical Research Letters*, 14(8), 808–811. <https://doi.org/10.1029/GL014i008p00808>
- Guiraud, R., Bellion, Y., Benkhelil, J., & Moreau, C. (1987). Post-Hercynian tectonics in Northern and Western Africa. *Geological Journal*, 22, 433–466. <https://doi.org/10.1002/gj.3350220628>
- Guiraud, M. (1990). Tectono-sedimentary framework of the early Cretaceous continental Bima formation (upper Benue Trough, NE Nigeria). *Journal of African Earth Sciences*, 10(1–2), 341–353. [https://doi.org/10.1016/0899-5362\(90\)90065-M](https://doi.org/10.1016/0899-5362(90)90065-M)
- Guiraud, R., & Maurin, J. C. (1992). Early Cretaceous rifts of Western and Central Africa: An overview. *Tectonophysics*, 213(1–2), 153–168. [https://doi.org/10.1016/0040-1951\(92\)90256-6](https://doi.org/10.1016/0040-1951(92)90256-6)
- Guiraud, R., & William, B. (1997). Implications to plate-scale tectonics Senonian basin inversion and rejuvenation of rifting in Africa and Arabia: Synthesis and implications to plate-scale. *Tectonics*, 282, 39–82. [https://doi.org/10.1016/S0040-1951\(97\)00212-6](https://doi.org/10.1016/S0040-1951(97)00212-6)
- Hammer, S. (1982). Airborne gravity is here! *Geophysics*, 48(3), 213–233. <https://doi.org/10.1190/1.1436758>
- Hildebrand, A. R., Pilkington, M., Connors, M., Ortiz-Aleman, C., & Chavez, R. E. (1995). Size and structure of the Chicxulub crater revealed by horizontal gravity gradients and cenotes. *Letters to Nature*, 376, 415–417. <https://doi.org/10.1038/376415a0>
- Hood, P., & Ward, S. H. (1969). Airborne geophysical methods. *Advances in Geophysics*, 13, 2–3. [https://doi.org/10.1016/S0065-2687\(08\)60508-7](https://doi.org/10.1016/S0065-2687(08)60508-7)
- Jacobsen, B. H. (1987). Case for upward continuation as a standard separation filter for potential-field maps. *Geophysics*, 52(8), 1138–1148. <https://doi.org/10.1190/1.1442378>
- Maurin, J. C., & Guiraud, R. (1993). Basement control in the development of the Early Cretaceous West and Central African rift system. *Tectonophysics*, 228, 81–95. [https://doi.org/10.1016/0040-1951\(93\)90215-6](https://doi.org/10.1016/0040-1951(93)90215-6)
- Nabighian, M. N., Grauch, V. J. S., Hansen, R. O., LaFehr, T. R., Li, Y., Peirce, J. W., Phillips, J. D., & Ruder, M. E. (2005). The historical development of the magnetic method in exploration. *Geophysics*, 70(6), 63–89. <https://doi.org/10.1190/1.2133784>
- Reid, A. B., Allsop, J. M., Granser, H., Millet, A. J., & Somerton, I. W. (1990). Magnetic interpretation in three dimensions using Euler deconvolution. *Geophysics*, 55(4), 80–91. <https://doi.org/10.1190/1.1442861>
- Wilson, M. (1992). Magmatism and rifting in Western and Central Africa from Late Jurassic to recent times. *Tectonophysics*, 213, 203–225. [https://doi.org/10.1016/0040-1951\(92\)90259-9](https://doi.org/10.1016/0040-1951(92)90259-9)
- Zeng, H., Xu, D., & Tan, H. (2007). A model study for estimating optimum upward-continuation height for gravity separation with application to a Bouguer gravity anomaly over a mineral deposit, Jilin province, northeast China. *Geophysics*, 72(4), 145–150. <https://doi.org/10.1190/1.2719497>